The affinity of azide for copper does not change significantly between the cobalt derivatives of the WT and of the SOD-Ile-137 mutant, being 154 and 175 M^{-1}, respectively. This may not hold for the zinc-copper derivatives if one should judge from the formation of the azide to copper charge transfer band, since values of 54 ± 15 M^{-1} for the mutant versus 93 ± 31 M^{-1} for the WT are obtained. The discrepancy revealed between the values obtained through NMR and electronic spectroscopy may arise not from intrinsic differences between the native and cobalt-substituted enzymes but from the different experimental conditions at which the titrations were performed, i.e., large differences in enzyme concentrations or changes in molar absorbance due to salt effects.

In the NMR experiment, the affinity values are obtained by simultaneous fitting of the azide dependence of the isotropic shifts of as many as 17 signals, and the results are very reliable. Accepting the latter values for our discussion, we may conclude that changing the residue 137 does not have an effect upon either the enthalpy or entropy contributions toward binding, despite the difference in the water structure inside the cavity and the copper coordination geometry.

In the study of another series of mutants[12] we have proposed that the charge inside the cavity determines the affinity of azide and of substrate (superoxide) for the protein, thus determining the enzymatic affinity. A close correlation between azide affinity and activity was found. In the present case, activity and anion affinity again appear to be closely interlinked.

Acknowledgment. This work has been performed with the contribution of the "Progetto Stategico Biotecnologie" of Italian CNR and of Chiron Corporation. The pulse radiolysis studies were supported under NIH Grant RO1 GM23656-10 and carried out at Brookhaven National Laboratory.

Registry No. SOD, 9054-89-1; L-Thr, 72-19-5; O_2^-, 11062-77-4; Cu, 7440-50-8; phosphate, 14265-44-2.

Mechanism and Products of Electrochemical Oxidation of 5,7-Dihydroxytryptamine

Glenn Dryhurst,* Agnes Anne,[1] Monika Z. Wrona, and D. Lemordant[2]

Contribution from the Department of Chemistry, University of Oklahoma, Norman, Oklahoma 73019. *Received March 18, 1988*

Abstract: It has been postulated that the mechanisms of electrochemical and autoxidation of the chemical neurotoxin 5,7-dihydroxytryptamine (5,7-DHT) are different. The former has been proposed to be a $2e^-,2H^+$ reaction leading to the corresponding *p*-quinone imine, while the latter has been proposed to be a $1e^-,1H^+$ reaction yielding a radical intermediate. The fundamental mechanism by which 5,7-DHT is oxidized is important because it is widely believed that the neurodegenerative effect of this compound is manifested by a reactive oxidation product formed in the central nervous system. The electrochemical oxidation of 5,7-DHT at low pH has been investigated. Contrary to earlier postulations, the initial step is a $1e^-,1H^+$ oxidation of 5,7-DHT to a radical intermediate. When electrolyses are performed at low applied potentials ($E_{p/2}$ for the first voltammetric oxidation peak of 5,7-DHT), several simple dimers are formed as ultimate reaction products. In view of the fact that the major dimer formed is 4,4′-bi-5,7-dihydroxytryptamine, it may be concluded that the predominant form of the radical intermediate is that in which the unpaired electron is located at the C(4) position. With increasingly positive applied potential the latter dimer is oxidized ($2e^-,2H^+$) to 4,4′-bi-[5-hydroxy-3-(2-aminoethyl)indolyliden-7-one]. However, at potentials greater than or equal to E_p for the first voltammetric oxidation peak, the primary radical is electrochemically oxidized ($1e^-,1H^+$) to the corresponding *p*-quinone imine. Nucleophilic attack by water yields 4,5,7-trihydroxytryptamine, which is rapidly further oxidized ($2e^-,2H^+$) to 5-hydroxytryptamine-4,7-dione.

5,7-Dihydroxytryptamine (5,7-DHT) is widely used for the selective chemical denervation of 5-hydroxytryptamine- (serotonin-) containing neurons.[3-10] The selectivity of 5,7-DHT is probably derived from its high-affinity uptake by the membrane pump of serotonergic neurons. It is rather generally believed that the neurodegenerative properties of 5,7-DHT result from an inherent chemical property, namely, ease of oxidation. Autoxidation of 5,7-DHT in vivo has been proposed to give reactive quinone imine species (**1**, **2**) which can alkylate nucleophiles such as neuronal membrane proteins as illustrated in Scheme I.[11] This reaction would, presumably, modify the neuronal membrane and, hence, denervate the neuron. The neurotoxicity of 5,7-DHT has also been speculated to be caused by interactions of intermediates **1** and **2** with the electron transport chain[10] or by the formation of cytotoxic reduced oxygen species ($O_2^{\bullet-}$, $HO^\bullet$, H_2O_2) as illustrated in Scheme I.[8,9,12,13,15]

Recently, Sinhababu and Borchardt[16] attempted to elucidate the mechanisms of both the autoxidation and electrochemical oxidation of 5,7-DHT. Autoxidation was found to be first order in terms of both O_2 and 5,7-DHT. This observation is consistent with a mechanism involving the incorporation of O_2 into the

(1) Laboratoire Chimie Analytique, Faculté Pharmacie, Université Paris V, 75270 Paris, France.
(2) Laboratoire d'Energétique et Réactivité aux Interfaces, Université P. et M. Curie, 75005, Paris, France.
(3) Baumgarten, H. G.; Björklund, A.; Lachemeyer, L.; Nobin, A.; Stenevi, U. *Acta Physiol. Scand., Suppl.* **1971**, *383*, 1-15.
(4) Baumgarten, H. G.; Evetts, K. D.; Holman, R. B.; Iverson, L. L.; Wilson, G. *J. Neurochem.* **1972**, *19*, 1587-1597.
(5) Baumgarten, H. G.; Björklund, A.; Lachenmeyer, L.; Nobin, A. *Acta Physiol. Scand., Suppl.* **1973**, *391*, 1-19.
(6) Serotonin Neurotoxins. Jacoby, J. L., Lytle, D., Eds. *Ann. N.Y. Acad. Sci.* **1978**, *305*, 1-702.
(7) Johnsson, G. *Annu. Rev. Neurosci.* **1980**, *3*, 169-187.
(8) Baumgarten, H. G.; Klemm, H. P.; Sievers, J.; Schlossberger, H. G. *Brain Res. Bull.* **1982**, *9*, 131-150.
(9) Baumgarten, H. G.; Jenner, S.; Björklund, A.; Klemm, H. P.; Schlossberger, H. G. In *Biology of Serotonergic Transmission*; Osborne, N. N., Ed.; Wiley: New York, 1982; Chapter 10.
(10) Johnsson, G. In *Handbook of Chemical Neuroanatomy*; Björklund, A., Hokfelt, T., Eds.; Elsevier: Amsterdam, 1983; Vol. 1, Methods in Chemical Neuroanatomy, Chapter XII, and references cited therein.
(11) Rotman, A.; Daly, J. W.; Crevelling, R. C. *Mol. Pharmacol.* **1976**, *12*, 887.
(12) Cohen, G.; Heikkila, R. E. *Ann. N.Y. Acad. Sci.* **1978**, *305*, 74-84.
(13) Baumgarten, H. G.; Klemn, H. P.; Lachenmeyer, L.; Björklund, A.; Lorenberg, N.; Schlossberger, H. G. *Ann. N.Y. Acad. Sci.* **1978**, *305*, 3-24.
(14) Klemm, H. P.; Baumgarter, H. G.; Schlossberger, H. G. *J. Neurochem.* **1980**, *35*, 1400-1408.
(15) Crevelling, C. R.; Rotman, A. *Ann. N.Y. Acad. Sci.* **1978**, *305*, 57-73.
(16) Sinhababu, A. K.; Borchardt, R. J. *J. Am. Chem. Soc.* **1985**, *107*, 7618-7626.

0002-7863/89/1511-0719$01.50/0

Scheme I

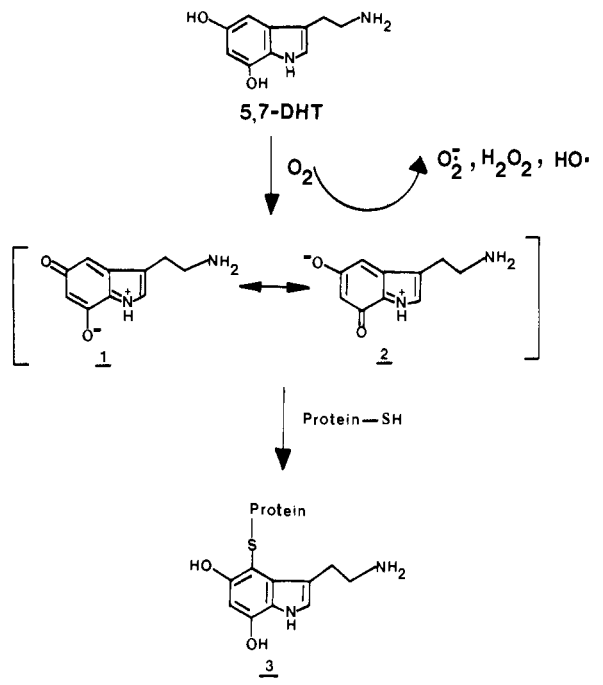

5,7-DHT nucleus and not consistent with the transformation of 5,7-DHT into quinones **1** and **2**. It was concluded that O_2 is initially incorporated into the C(4) position of 5,7-DHT to give a free radical superoxide complex. According to Sinhababu and Borchardt,[16] the key step in the autoxidation process is formation of free radical **5** although direct evidence for such an intermediate was not obtained.

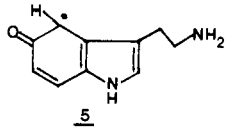

Results from cyclic voltammetry studies in supporting electrolyte solutions ranging from 0.1 M H_2SO_4 to pH 7.4 phosphate buffer were interpreted to show that the primary electrochemical oxidation product of 5,7-DHT is *p*-quinone imine **1**/**2**. Unfortunately, however, the latter species could not be detected by fast-sweep cyclic voltammetry because it was, presumably, too short-lived. Cyclic voltammograms of 5,7-DHT dissolved in 0.1 M H_2SO_4 showed that after scanning through the first voltammetric oxidation peak a reversible reduction peak could be observed on the reverse sweep at ~0.0 V vs Ag/AgCl. This peak was assumed to be caused by reduction of the *p*-quinone of 4,5,7-trihydroxytryptamine (4,5,7-THT), although these compounds were not isolated and identified.

Many unanswered questions therefore remain concerning the oxidation chemistry of the neurotoxin 5,7-DHT and how this chemistry relates to its neurodegenerative properties. This report focuses on the electrochemical oxidation of 5,7-DHT at low pH primarily because, according to Sinhababu and Borchardt,[16] only under such conditions does the electrochemical oxidation lead to a voltammetrically detectable intermediate/product. The objectives of the work were to ascertain if the initial oxidation step is a 1e reaction giving a radical intermediate or a 2e reaction leading to a quinone imine intermediate. Because the putative radical intermediate is too reactive to be detected by fast-sweep cyclic voltammetry[16] and therefore by ESR spectroscopy, it was believed that the existence of such an intermediate could best be established by the isolation and structural characterization of key products of the oxidation reaction.

Experimental Section

5,7-Dihydroxytryptamine (creatinine sulfate salt) was obtained from Sigma (St. Louis, MO). Conventional equipment was employed for all electrochemical studies.[17] A pyrolytic graphite electrode (PGE, Pfizer Minerals, Pigments and Metals Division, Easton, PA) having an approximate surface area of 4 mm^2 was used for voltammetry. All voltammograms were corrected for *IR* drop. Controlled-potential electrolyses and coulometry employed plates of pyrolytic graphite as the working electrode. Information about typical electrochemical cells is presented elsewhere.[18,19] However, prior to adding 5,7-DHT into the working electrode compartment of an electrochemical cell, the supporting electrolyte solution was always thoroughly deoxygenated by vigorously bubbling nitrogen gas. This gas stream was maintained throughout the course of all controlled-potential electrolyses. All potentials are referred to the saturated calomel reference electrode (SCE) at ambient temperatures (23 ± 3 °C).

High-performance liquid chromatography (HPLC) was performed with a Gilson System 42 equipped with dual pumps, an Apple IIe controller, and a Rheodyne Model 7125 loop injector (normally a 2.0-mL loop was employed). A Gilson Holochrome variable-wavelength detector was used, which was generally set at 254 nm. HPLC separations normally employed a reversed-phase column (Brownlee Laboratories; RP-18, 5 μm, 25 × 0.7 cm). A short guard column (Brownlee Laboratories; RP-18, 5 μm, OD-GU, 5 × 0.5 cm) was always used. HPLC separations were carried out with the following mobile phases: Solvent A was prepared by adding 8.0 mL of MeOH and 7 mL of concentrated ammonia to approximately 700 mL of water. After thoroughly mixing, the resulting solution was diluted to 800 mL with water. The solution was then adjusted to pH 3.77 by addition of concentrated formic acid (Aldrich, 96% ACS reagent grade). Solvent B was HPLC grade (Fisher) methanol. The following conditions were employed to effect HPLC separations: 0–35 min, 100% solvent A; 35–90 min, a linear gradient from 0% solvent B to 50% solvent B. The flow rate was 2 mL min^{-1}, and normally, 2.0 mL of the electrolysis product solution was injected. For preparative purposes the products eluted under each chromatographic peak were combined. Generally, several days were needed to collect a sufficient quantity of even the major product species to permit spectral structure elucidations to be carried out. Product solutions were desalted (i.e., ammonium formate removed) by using a reversed-phase column of the same type used for the usual separation but which has lost much of its activity. The column was initially flushed with water at a flow rate of 3 mL min^{-1}. The sample (2 mL) dissolved in pH 3.77 aqueous ammonium formate/methanol was then injected. After ~3 min a small peak due to ammonium formate appeared. At this point a second 2-mL injection of the sample was made. This was repeated one or two more times. Approximately 2–3 min after the final ammonium formate peak appeared the solvent was changed to H_2O/MeOH (80:20, v/v) adjusted to pH 2.4 with concentrated HCl. The sample peak then usually emerged after 8–10 min and was collected. The mobile phase was then changed back to water and the procedure repeated. The resulting solution containing the desalted product was shell frozen and freeze-dried. The purity of all products obtained in this way was always checked by HPLC analysis using the usual procedure.

High-performance liquid chromatography–mass spectrometry (LC–MS) was performed on a Kratos Model MS 25/RFA instrument equipped with a thermospray source. For these experiments, an analytical column was employed (Brownlee Laboratories; RP-18, 5 μm, 25 × 0.4 cm) and only HPLC solvent A was used. The mobile-phase flow rate was 0.9 mL min^{-1}. Under these conditions, the retention times (t_R) of most of the peaks were approximately the same as those observed with the semipreparative column at a flow rate of 2 mL min^{-1} described earlier. In many LC–MS experiments a Waters Model 400 UV detector (254 nm) was interposed between the exit of the HPLC column and the entrance to the thermospray system so that the UV vs time response could be compared to the total ion current vs time response observed with the mass spectrometer. Typically, the thermospray capillary tip was maintained at ca. 190 °C and the source temperature at ca. 240 °C. Low- and high-resolution fast atom bombardment mass spectrometry (FAB-MS) was carried out on a VG Instruments ZAB-E spectrometer. Electron impact (EI-) MS was carried out with a Hewlett-Packard Model 5985B mass spectrometer. ^1H NMR spectra were recorded on a Varian Model XL-300 (300-MHz) spectrometer. Infrared spectra were obtained with a Mattson Model Sirius 100 FT-IR spectrometer. UV–visible spectra were recorded on a Hitachi 100-80 spectrophotometer.

All electrolyses were carried out in water adjusted to pH 1.5 with HCl. In a typical electrolysis, 15–20 mg of 5,7-DHT creatinine sulfate (MW = 403.4) was added to 35 mL of deoxygenated pH 1.5 HCl contained

(17) Owens, J. L.; Marsh, H. A.; Dryhurst, G. *J. Electroanal. Chem. Interfacial Electrochem.* **1978**, *91*, 231–247.
(18) Wrona, M. Z.; Lemordant, D.; Lin, L.; Blank, C. L.; Dryhurst, G. *J. Med. Chem.* **1986**, *29*, 499–505.
(19) Wrona, M. Z., Dryhurst, G. *J. Org. Chem.* **1987**, *52*, 2817–2825.

in the working electrode compartment of an electrolysis cell. The resulting solution (ca. 1–1.5 mM 5,7-DHT) was then electrolyzed at two plates of pyrolytic graphite (total area ca. 80 cm^2). When the electrooxidation was complete as judged by cyclic voltammetry, UV–visible spectra, and HPLC analysis, the product solution was separated by HPLC with repeated 2-mL injections. As each component eluted, it was collected in a freeze-drying flask maintained at about −80 °C (dry ice). The combined product solution contained in such flasks was not melted until additional purification or desalting was carried out. It might be noted that if the crude product solution was freeze-dried to concentrate the components, HPLC analysis showed that additional products were formed. Detailed spectral and electrochemical information about key major oxidation products of 5,7-DHT is presented below.

5-Hydroxytryptamine-4,7-dione (H). **H** was isolated as a deep orange solid. In pH 1.5 HCl the spectrum of the orange solution of **H** showed λ_{max} = 461, 338, 283, and 225 nm (Figure 8B). At pH 7.0 the solution of **H** became pink [λ_{max} = 512, 337 (sh), 292, 232 nm]. Cyclic voltammetry of **H** in pH 1.5 HCl showed a reversible reduction peak at −0.07 V and an apparently irreversible oxidation peak at 0.97 V (Figure 8A). Reduction of **H** by controlled potential electrolysis at −0.15 V in pH 1.5 HCl gave a colorless solution (λ_{max} = 287, 250, 210 nm). This is the spectrum of 4,5,7-THT.

FAB-MS of **H** [thioglycerol (TG) matrix] gave the following major peaks: *m/e* (relative abundance) 207 (MH^+, 60), 315 (M + TGH^+, 100), 423 (M + TG_2H^+, 4), 529 (M + $C_9H_{23}O_6S_3^+$, 6). These spectral data clearly indicate that the pseudomolecular ion of **H** (MH^+) has a molar mass of 207 g. High-resolution FAB-MS on the latter ion gave an accurate *m/e* = 207.0784 which corresponds to the formula $C_{10}H_{11}N_2O_3$ (theory 207.0767). EI-MS (12 eV, 220 °C) on **H** gave the following results: *m/e* (relative abundance) 208 (0.5), 207 (0.6), 206 (M^+, 1.0), 192 (1.2), 191 (11.5), 190 (M^+ − NH, 100), 189 (19.5), 188 (M^+ − H_2O, 23.2), 187 (4.4), 186 (21.7), 178 (1.5), 177 (M^+ − $CHNH_2$, 12.2), 175 (3.9), 174 (14.9), 163 (2.0), 162 (M^+ − $CH_2CH_2NH_2$, 13.3), 161 (8.7), 160 (6.7). The IR spectrum of **H** (KBr pellet) showed the following bands (cm^{-1}): 2860–3160 (br and strong, O–H and N–H stretches), 1640 (s, C=O), 1610 (s, sh), 1480 (m), 1370 (s), 1350 (m), 1300 (w), 1275 (w), 1235 (w), 1195 (w), 1120 (w), 1040 (w), 965 (m), 910 (w), 840 (w), 810 (m), 765 (m), 710 (m). These MS and IR spectral data indicate that **H** has a molar mass of 206 g and an elemental formula $C_{10}H_{10}N_2O_3$ and that it contains carbonyl and hydroxyl groups. In addition, the EI-MS indicates that the ethylamine ($CH_2CH_2NH_2$) side chain of 5,7-DHT remains.

Before discussing the ^1H NMR spectrum of **H** it is of value to summarize that of 5,7-DHT (300 MHz, Me_2SO-d_6): δ 10.44 (d, *J* = 1.8 Hz, 1 **H**, N(1) H), 7.7 (very br, s, 5 H, NH_3^+, 2 **OH**), 6.99 (d, *J* = 2.4 Hz, C(2) **H**), 6.28 (d, *J* = 2.1 Hz, 1 H, C(4) **H**), 6.13 (d, *J* = 1.8 Hz, 1 H, C(6) H), 2.98 (t, 2 H, CH_2), 2.86 (t, 2 H, CH_2). Addition of D_2O to the above solution caused the peaks at 10.44 and 7.7 ppm to disappear and the doublet at 6.99 ppm to collapse into a singlet. The peak assignments were based upon comparisons of the above NMR spectra with that of 5-hydroxytryptamine,[18] previous partial interpretations of the spectrum of 5,7-DHT in D_2O,[16,20] and homonuclear decoupling experiments. The ^1H NMR spectrum of **H** in Me_2SO-d_6: δ 12.51 (s, 1 H, N(1) H), 11.20 (br s, 1 H, OH), 8.01 (br s, 3 H, NH_3^+), 7.04 (d, *J* = 2.7 Hz, 1 H, C(2) H), 5.73 (s, 1 H, C(6) H), 3.05 (t, 2 H, CH_2), 2.95 (t, 2 H, CH_2). Addition of D_2O caused the resonances at 12.51, 11.20, and 8.01 ppm to disappear and the doublet at 7.04 ppm to collapse into a singlet. The absence of a resonance for C(4)–H in **H** and the appearance of the C(6)–H as a singlet, rather than a doublet as in 5,7-DHT, indicates that a carbonyl group occupies the C(4) position. These spectral data thus suggest that **H** is 5-hydroxytryptamine-4,5-dione. The UV–visible spectrum of **H** is quite similar to that of 1,4-benzoquinone and 2-hydroxy-1,4-naphthoquinone but very different from that of 1,2-benzoquinone,[21] which provides strong support for the structure **H**.

4,4′-Bi-[5-hydroxy-3-(2-aminoethyl)indolyliden-7-one] (G). Compound **G** was isolated as a bright yellow solid which exhibited a very characteristic UV–visible spectrum [λ_{max} in dilute HCl pH 2.0 = 378, 355 (sh), 302, 274 (sh), 228 nm; Figure 6A]. Cyclic voltammograms of **G** at pH 1.5 show that it is reduced via a single, sharp reduction peak (R_2) at −0.59 V (Figure 6B). Having scanned through this peak the product formed showed a reversible oxidation–reduction couple (peaks O_2'/R_1') at 0.10 V. FAB-MS of G in a thioglycerol (TG) matrix gave an intense pseudomolecular ion at *m/e* = 381 along with small but significant ions at *m/e* = 489 (M + TGH^+) and 597 (M + 2TG + H^+). Accurate mass measurements (thioglycerol + glycerol matrix) on the pseudomolecular ion gave *m/e* = 381.1577 ($C_{20}H_{21}N_4O_4$, calcd *m/e* = 381.1563). Thus, **G** has a molar mass of 380 g and a molecular formula $C_{20}H_{20}N_4O_4$. IR spectrum (film on KBr plate, cm^{-1}): 3429 (br, s, O–H, N–H stretches), 2915 (br, s, aliphatic C–H stretches), 1653 (m, C=O), 1620 (s, C=O), 1585 (s), 1545 (w), 1510 (m), 1500 (w), 1480 (w), 1460 (m), 1450 (m), 1440 (w), 1400 (s), 1376 (w), 1365 (w), 1350 (m), 1310 (w), 1270 (w), 1233 (m), 1197 (m), 1165 (m), 1122 (m), 1095 (s), 1070 (s).

^1H NMR spectrum (Me_2SO-d_6): δ 12.60 (d, *J* = 2.1 Hz, 1 H, N(1) H), 12.12 (d, *J* = 2.4 Hz, 1 H, N(1′) H), 8.06 (br s, ca. 4 H, NH_3^+, OH), 7.80 (br s, ca. 4 H, NH_3^+, OH), 7.32 (d, *J* = 2.7 Hz, 1 H, C(2) H), 7.12 (d, *J* = 2.4 Hz, 1 H, C(2′) H), 5.64 (s, 1 H, C(6) H), 2.98 (br m, ca. 6 H), 2.55 (br m, ca. 4 H). Addition of D_2O to the above sample caused the peaks at 12.60, 12.12, 8.06, and 7.80 ppm to disappear and the doublets at 7.32 and 7.12 ppm to collapse into singlets.

The FAB-MS results indicate that **G** (molar mass 380 g) must be some form of oxidized dimer of 5,7-DHT (molar mass 192 g). ^1H NMR spectra clearly slow that the two indolic residues are different since separate signals are observed for the indolic N(1)–H and C(2)–H protons. In addition, two distinct signals due primarily to the exocyclic NH_3^+ are observed. The principal clue to the structure of **G** from NMR spectra is provided by the singlet at 5.64 ppm due to a single proton. This singlet occurs at a very similar chemical shift to that of the C(6)–H proton of H (5.73 ppm) and hence these protons must occur in similar structural environments. The two sets of multiplets observed at 2.98 and 2.55 ppm must be due, in part, to contributions from two side chain CH_2CH_2 groups (see discussion of the NMR spectrum of 5,7-DHT). One of these multiplets (2.98 ppm) integrated approximately 30% greater than the other (2.55 ppm). This suggests that the former signal contains contributions from two more protons. The methylene moiety located at the C(6′) position in structure G_4 (Scheme II) thus contributes to the multiplet at 2.98 ppm.[20] Structure G_4 is only one of several tautomers of **G** (Scheme II). However, the ^1H NMR spectrum clearly supports the conclusion that in Me_2SO the predominant species in solution is G_4.

4,4′-Bi-[3-(2-aminoethyl)indolyliden-7-one] 5,5′-Ether (12). Compound **12** was prepared by controlled-potential electrochemical reduction of **G** (ca. 3 mg), dissolved in 35 mL of pH 1.5 HCl, at the PGE at −0.75 V. As the reduction proceeded, the bright yellow color of **G** faded and the solution became colorless [λ_{max} = 359, 343, 328 (sh), 276 nm; Figure 7A]. The solution was then electrochemically oxidized at 0.15 V when a deep yellow-orange color appeared [λ_{max} = 434, 403, 386 (sh), 260 nm; Figure 7B]. Direct injection of a 2-mL aliquot of this solution, via a loop injector, into the thermospray mass spectrometer system with 0.1 M aqueous ammonium acetate as the mobile phase gave a single peak (MH^+) at *m/e* = 363. Thus **12** has a molar mass of 362 g. The yellow solution of **12** was freeze-dried, and the resulting orange solid was dissolved in ca. 2 mL of H_2O/MeOH (9:1, v/v), adjusted to pH 2 with HCl, and passed through a column of Sephadex LH-20 with the latter solvent as the mobile phase at a flow rate of ~20 mL h^{-1}. The bright yellow-orange band was collected and freeze-dried. FAB-MS (dithiothreitol/dithioerythritol matrix) gave intense ions at *m/e* = 363 (MH^+) and 365 ($MH_2{\cdot}H^+$). Accurate mass measurements on the former ion gave *m/e* = 363.1465 ($C_{20}H_{19}N_4O_3$, calcd *m/e* = 363.1457). A cyclic voltammogram of **12** in pH 1.5 HCl showed a reduction peak at E_p = 0.06 V (R_1') and, on the reverse sweep, a quasi-reversible oxidation peak at E_p = 0.10 V (O_2') (Figure 7C). ^1H NMR (Me_2SO-d_6): δ 12.56 (s, 2 H, N(1) H and N(1′) H), 7.73 (s, 6 H, 2 NH_3^+), 7.28 (d, *J* = 2.4 Hz, 2 H, C(2) H and C(2′) H), 6.08 (s, 2 H, C(6) H and C(6′) H). Addition of a few drops of D_2O to the above solution caused the peaks at 12.56 and 7.73 ppm to disappear and the doublet at 7.28 ppm to collapse into a singlet. These spectral data are compatible with the highly symmetrical structure **12** (Scheme III).

Results

Linear Sweep and Cyclic Voltammetry. Voltammograms of 5,7-DHT at the PGE at pH 1.5 show three oxidation peaks, O_1, O_2, and O_3 (Figure 1). The experimental peak current function ($i_p/AC\nu^{1/2}$) for oxidation peak O_1 increases with increasing sweep rate, ν. For example, with 0.15 mM 5,7-DHT, $i_p/AC\nu^{1/2}$ systematically increases from 2.5 × 10^3 to 14.8 × 10^3 μA cm^{-2} mM^{-1} L $V^{-1/2}$ $s^{1/2}$ over a sweep rate range of 10–500 mV s^{-1}. The value of $i_p/AC\nu$, however, remained constant at 2.3 ± 0.6 × 10^4 μA cm^{-2} mM^{-1} L V^{-1} s over the same sweep rate range. These data indicate that peak O_1 is due to the electrochemical oxidation of 5,7-DHT to adsorbed product(s).[23] Addition of tetrabutyl-

(20) Schlossberger, H. G. In Serotonin Neurotoxins. *Jacoby*, J. H., Lytle, L. D., Eds. *Ann. N.Y. Acad. Sci.* **1978**, *305*, 25–35.

(21) Britton, G. *The Biochemistry of Natural Pigments*; Cambridge University Press: New York, 1983; pp 74–81.

(22) Silverstein, R. M.; Bassler, G. C.; Morrill, T. C. *Spectrometric Identification of Organic Compounds*, 4th ed.; Wiley: New York, 1981.

(23) Wopschall, R. H.; Shain, I. *Anal. Chem.* **1967**, *39*, 1514–1527.

Scheme II

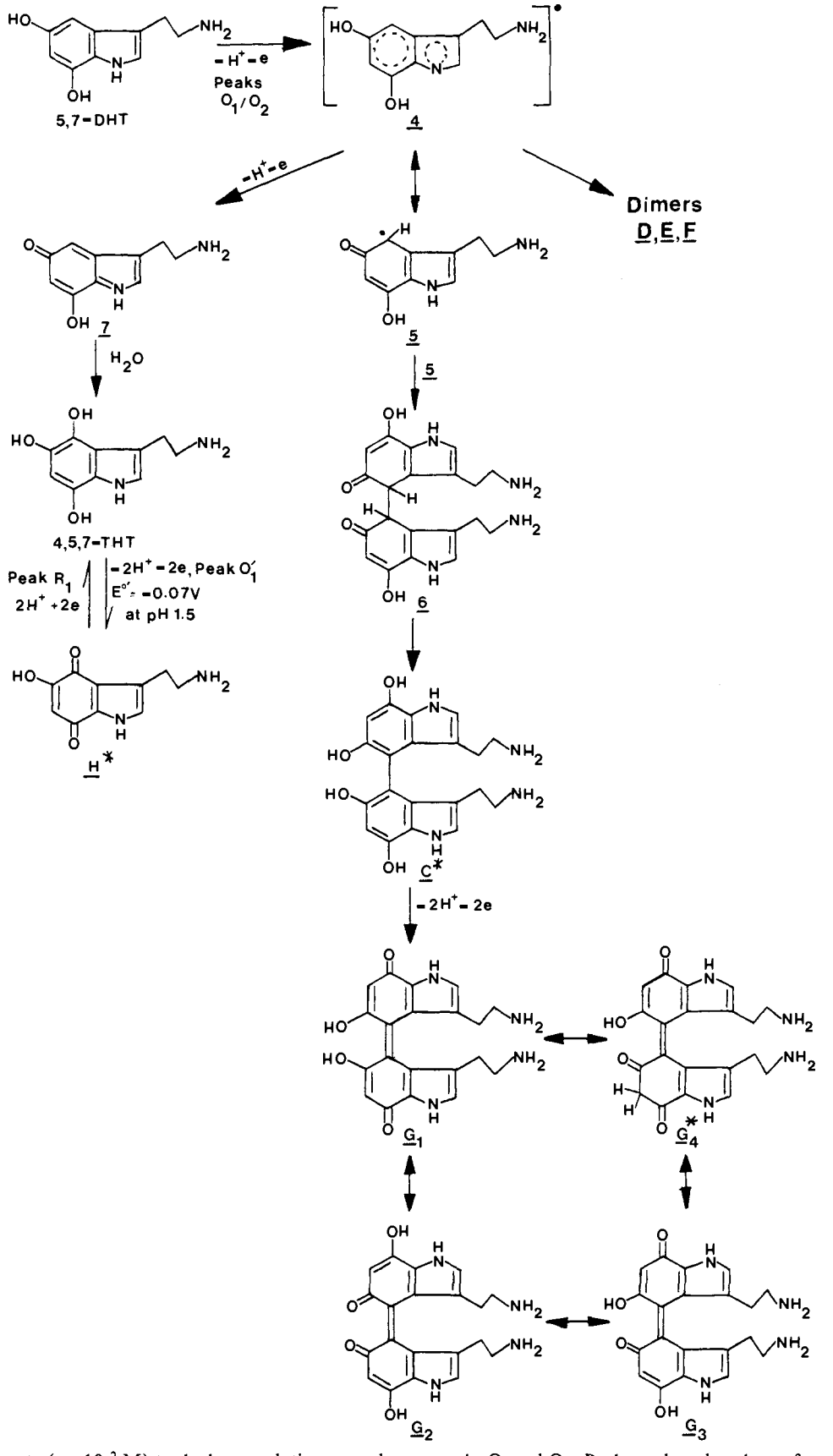

ammonium perchlorate (ca. 10^{-2} M) to the latter solution caused peaks O_1 and O_2 to collapse into a single peak. The experimental peak current function for this peak was constant at 1.47 ± 0.03 × 10^3 μA cm^{-2} mM^{-1} L V$^{-1/2}$ s$^{1/2}$ over the sweep rate range 10–500 mV s^{-1}. At higher bulk solution concentrations of 5,7-DHT, addition of TBAP did not result in a simple merger of oxidation peaks O_1 and O_2. Rather, a broad peak was formed between about 0.3 and 0.6 V which was clearly composed of at least two or three superimposed peaks. These peaks result from both adsorption effects and the fact that in the vicinity of peaks O_1 and O_2 more than one concentration-dependent electrode reaction occurs (see later Discussion). All subsequent experiments that will be de-

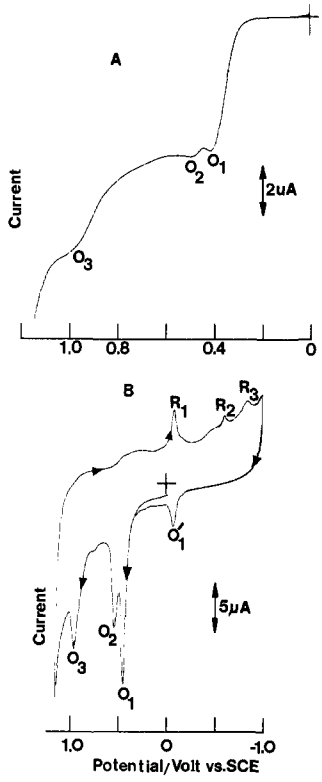

Figure 1. Linear sweep and cyclic voltammograms at the PGE of (A) 1 mM and (B) 0.1 mM 5,7-dihydroxytryptamine dissolved in water adjusted to pH 1.5 with HCl. Sweep rate: (A) 5 mV s^{-1}; (B) 200 mV s^{-1}.

Scheme III

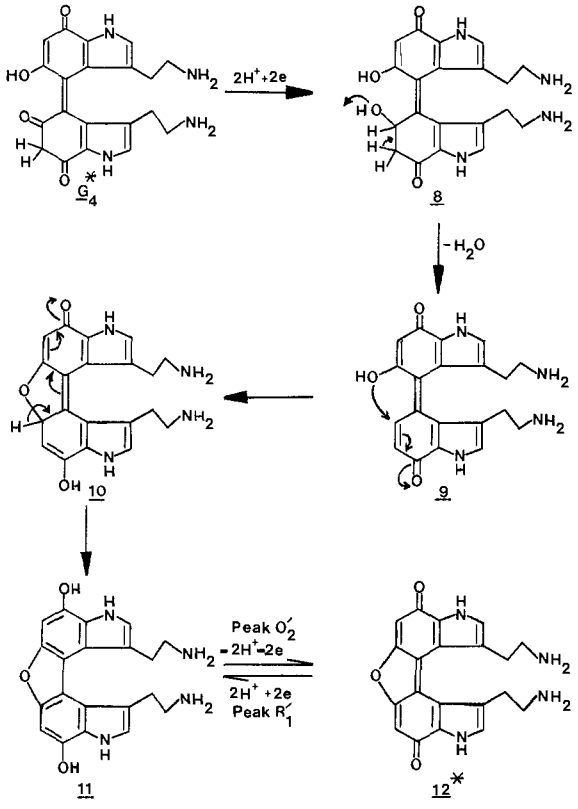

scribed were carried out in the absence of TBAP or other added surfactants.

A cyclic voltammogram of 5,7-DHT at pH 1.5 (Figure 1B) shows that having scanned through oxidation peaks O_1, O_2, and O_3 three reduction peaks, R_1, R_2, and R_3, can be observed on the

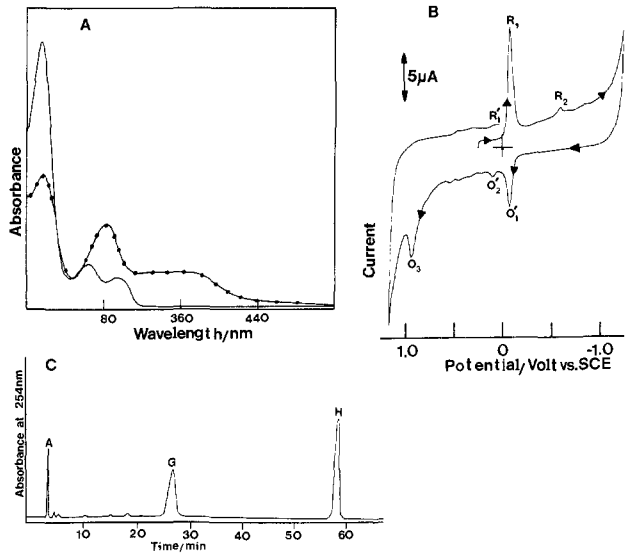

Figure 2. (A) Spectrum of 85 μM 5,7-dihydroxytryptamine in pH 1.5 HCl (—) before electrolyses and (●) after exhaustive electrolysis at 0.40 V at a pyrolytic graphite electrode. (B) Cyclic voltammogram at the PGE of the product solution from (A). Sweep rate, 200 mV s^{-1}. (C) HPLC chromatogram of the product solution from (A). See Experimental Section.

reverse sweep. Reduction peak R_1 forms a quasi-reversible couple with oxidation peak O_1' observed on the second anodic sweep. Peaks R_1, R_2, and R_3 are observed if the initial anodic sweep is reversed after scanning through peaks O_1 and O_2.

Adsorption peak O_1 is only observed at pH <3. At pH 1.5 and 2.1 the peak potential (E_p) for peak O_1 is 0.41 and 0.32 V, respectively. E_p values for oxidation peak O_2 at pH 1.5, 2.1, 3.2, 4.1, 5.2, 7.0, 7.9, and 9.1 are 0.49, 0.46, 0.32, 0.34, 0.19, 0.085, 0.016, and −0.053 V, respectively. Thus, 5,7-DHT is electrochemically oxidized via the peak O_1 and peak O_2 processes in pH-dependent reactions. However, detailed information about reaction products has been obtained following electrooxidations only at pH 1.5.

Controlled-Potential Electrolyses. Controlled-potential electrooxidations of 5,7-DHT at 0.40 V (E_p for peak O_1) in pH 1.5 HCl gave concentration-dependent n values. For example, exhaustive electrooxidation of 18–20 μM solutions of 5,7-DHT gave experimental n values of 3.5 ± 0.2. Electrooxidations of 2 mM solutions of 5,7-DHT gave n = 2.6 ± 0.3. Figure 2A shows the spectral changes that accompany the controlled-potential electrooxidation of 85 μM 5,7-DHT at 0.40 V. Thus, the characteristic spectrum of 5,7-DHT (λ_{max} in pH 1.5 HCl: 294, 264, 216 nm) disappears and is replaced by a product spectrum that shows a broad band between 460 and 310 nm and well-defined bands at λ_{max} = 283 and 216 nm. A cyclic voltammogram of the product solution (Figure 2B) shows a large quasi-reversible reduction peak (peaks R_1/O_1' couple) at −0.07 V and a much smaller reduction peak R_2 at −0.59 V. Oxidation peak O_3 (E_p = 0.95 V) could be observed without initially scanning through reduction peaks R_1 and R_2. HPLC analysis of the product solution showed three major chromatographic peaks, A, G, and H (Figure 2C). Chromatographic peak A is due to creatinine and will not be discussed further. With increasing concentrations of 5,7-DHT oxidized the long-wavelength band in the spectrum of the product solution (Figure 2A) grows systematically larger. Simultaneously, reduction peak R_2 in cyclic voltammograms of the product solution becomes larger, as does HPLC peak G. Thus, electrooxidations of 5,7-DHT at E_p for peak O_1 (0.40 V) yields two major products responsible for HPLC peaks G and H; these will be referred to as compounds **G** and **H**. With increasing concentrations of 5,7-DHT oxidized the experimental n value decreases somewhat, as noted earlier, and the relative yield of **G** systematically increases.

As the potential employed to oxidize 5,7-DHT was made more positive (0.6 V was the most positive potential investigated), the electrolysis proceeded more rapidly. HPLC analysis of the product

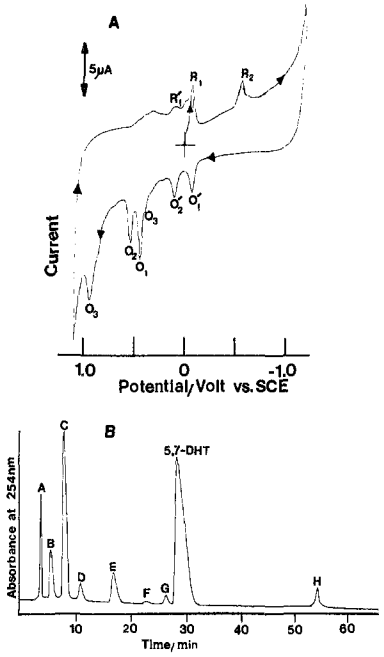

Figure 3. (A) Cyclic voltammogram at the PGE of the solution obtained after controlled-potential electrooxidation of 0.1 mM 5,7-dihydroxytryptamine in pH 1.5 HCl at 0.34 V for 12 h. Sweep rate, 200 mV s^{-1}. (B) HPLC chromatogram of the solution obtained after controlled-potential electrooxidation of 1.05 mM 5,7-dihydroxytryptamine in pH 1.5 HCl at 0.34 V for 12 h. Chromatographic conditions are given in the Experimental Section.

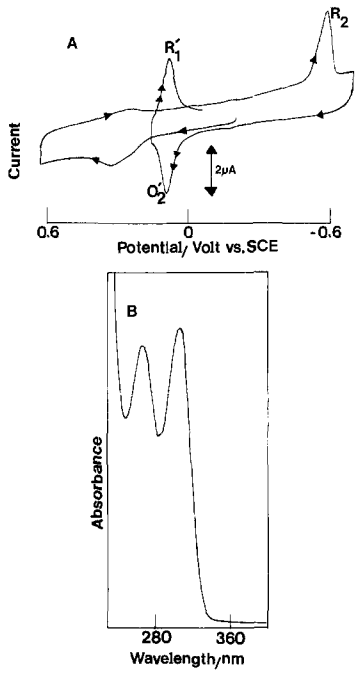

Figure 4. Cyclic voltammogram at the PGE of 4,4'-bi-5,7-dihydroxytryptamine (**C**) at pH 1.5. Sweep rate, 100 mV s^{-1}. (B) UV spectrum of **C** at pH 3.77.

solutions showed that as the applied potential was made more positive the relative yield of **H** increased while that of **G** decreased. In addition, for any given concentration of 5,7-DHT oxidized (0.02–2 mM), experimental n values increased with increasingly positive potential. The limiting n value (3.8 ± 0.2) was observed when very low concentrations of 5,7-DHT (20 μM) were oxidized at high potential (0.6 V). HPLC analysis of the resulting product solution showed only traces of **G**; **H** was the major product.

Controlled-potential electrolyses of 5,7-DHT at potentials $<E_p$ for peak O_1 gave more complex results. Electrolyses at 0.34 V (ca. $E_{p/2}$ for peak O_1) were quite slow, and at this potential it was not possible to oxidize all 5,7-DHT even after 24 h. However, a cyclic voltammogram of a partially oxidized solution (Figure 3A) showed, on the first cathodic sweep, reduction peaks R_1 (−0.07 V) and R_2 (−0.59 V). On the reverse sweep oxidation peak O_1' appeared, which formed a quasi-reversible couple with peak R_1. Oxidation peak O_2' (0.11 V) forms a reversible couple with reduction peak R_1', observed on the second cathodic sweep. The peaks O_2'/R_1' couple cannot be observed unless reduction peak R_2 is first scanned. Oxidation peaks O_1, O_2, and O_3 observed in Figure 3A are due to unoxidized 5,7-DHT. Several additional small oxidation peaks can be observed in Figure 3A, the most noticeable being peak O_3' (0.38 V). This peak is observed without initially scanning peaks R_1 and R_2. The cyclic voltammogram shown in Figure 3A was recorded following partial electrochemical oxidation of 100 μM 5,7-DHT at 0.34 V. Following electrolyses of higher concentrations of 5,7-DHT, cyclic voltammograms were similar to that shown in Figure 3A except that reduction peak R_2 became larger relative to peak R_1. HPLC analysis of the product mixture obtained after partial oxidation of 1 mM 5,7-DHT gave the result shown in Figure 3B. Thus seven products, **B–H**, are observed. Following the electrooxidation of 0.1 mM 5,7-DHT at 0.34 V, a similar chromatogram was obtained.

Characterization of Oxidation Products. The results described above indicate that oxidation of 5,7-DHT in pH 1.5 HCl at a potential greater than or equal to E_p for peak O_1 results in the formation of two major products, **G** and **H**. The more positive the applied potential the larger the relative yield of **H**. Electrolyses at potentials ca. $E_{p/2}$ for peak O_1 yields **C** as the major product (Figure 3B) along with smaller amounts of **B** and **D–H**.

Only compounds **G** and **H** were sufficiently stable to permit their isolation and the application of spectral methods for structure elucidation. Information about compounds **B–F** was largely derived from their UV–visible spectra, electrochemistry, and LC–MS behaviors.

The spectrum of **B** dissolved in the HPLC mobile phase (pH 3.77) showed a band at λ_{max} = 300 nm along with a small, ill-defined shoulder extending from ~330–440 nm. Over the course of 2 days at room temperature in the presence of air, the long-wavelength shoulder grew appreciably and the solution became yellow. Because of the instability of **B** attempts to isolate and desalt it were unsuccessful. LC–MS also failed to give useful information concerning the structure of **B**.

C exhibited a very characteristic spectrum (λ_{max} at pH 3.77 = 308, 268 nm; Figure 4B). However, shortly after collection the colorless solution of **C** began to turn yellow. Ultimately, the spectrum of the bright yellow solution became identical with that of **G**. A cyclic voltammogram of **C** at pH 1.5 (Figure 4A) shows a rather broad oxidation peak at ca. 0.35 V. The concentration of **C** used to obtain the voltammogram shown in Figure 4A is not known. However, with increasing concentration the oxidation peak shifted to more positive potentials. Having scanned through the oxidation peak of **C** a well-defined reduction peak, R_2, appeared on the reverse sweep at −0.59 V. On the subsequent potential sweeps quasi-reversible peaks O_2'/R_1' appear (Figure 4A). Reduction peak R_2 and the quasi-reversible peaks O_2'/R_1' are characteristic of compound **G**. Controlled-potential electrooxidation of **C** at 0.40 V at pH 1.5 resulted in its quantitative conversion into **G** (UV–visible spectra, HPLC analysis). LC–MS on a fresh sample of **C** showed an intense pseudomolecular ion (MH^+) at m/e = 383. Thus, **C** (molar mass 382 g) must be a simple dimer of 5,7-DHT (molar mass 192 g).

D was always a minor oxidation product of 5,7-DHT. As with **C**, the spectrum of **D** showed characteristic double bands (λ_{max} at pH 3.77 = 294, 280 nm) suggesting that it is also a dimeric compound. In the presence of air the spectrum of **D** changed over the course of a few hours (λ_{max} at pH 3.77 = 364, 302, 258 nm). Because of its instability and the low concentrations of **D** that could be collected, it was not possible to obtain either cyclic voltammograms or useful LC–MS data.

A freshly collected sample of **E** also showed characteristic double peaks in its UV spectrum (λ_{max} at pH 3.77 = 294, 280 nm; Figure 5A) which were similar to those of products **C** and

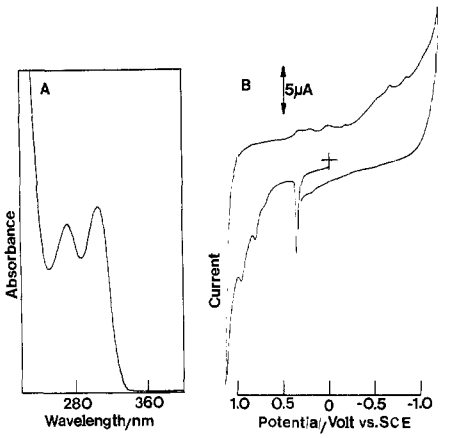

Figure 5. (A) UV spectrum of dimer **E** at pH 3.77. (B) Cyclic voltammogram at the PGE of **E** at pH 1.5. Sweep rate, 200 mV s^{-1}.

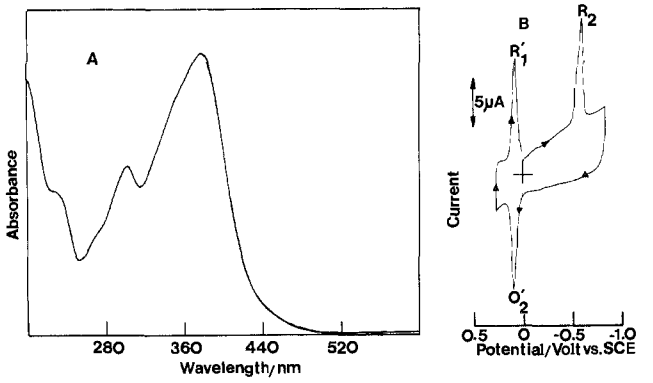

Figure 6. (A) Spectrum and (B) cyclic voltammogram at the PGE of 4,4′-bi-5-hydroxyindolyliden-7-one **G** in water adjusted to pH 1.5 with HCl. Sweep rate in (B), 200 mV s^{-1}.

D. As with the latter compounds, a colorless solution of **E** was slowly air oxidized to give a yellow solution (λ_{max} at pH 3.77 = 380, 302, 272 nm). HPLC analysis showed that **E** was air oxidized to two major products at t_R = 6.0 and 8.0 min. Both of these products had the same spectrum (λ_{max} at pH 3.77 = 380, 302, 272 nm). A cyclic voltammogram of **E** at pH 1.5 (Figure 5B) shows a very sharp oxidation peak at 0.36 V. LC–MS showed an intense pseudomolecular ion (MH^+) at m/e = 383, indicating that **E** is a simple dimer (molar mass 382 g) of 5,7-DHT.

The very minor product **F** gave a UV spectrum (λ_{max} at pH 3.77 = 306, 271 nm) similar to those of **C**–**E**. Compound **F** also decomposed (oxidized) when its solution was allowed to stand in the air. LC–MS showed that **F** gave a pseudomolecular ion at m/e = 383. However, samples of **F** obtained by HPLC separation were too dilute to permit cyclic voltammograms to be recorded. Nevertheless, UV spectra and LC–MS results indicate that **F** is probably a dimer of 5,7-DHT.

As was noted in earlier discussion, yellow **G** is formed as a result of the electrochemical (or air) oxidation of dimer **C** (molar mass 382 g). Oxidations of relatively high concentrations (ca. 1 mM) of 5,7-DHT at potentials corresponding to E_p for peak O_1 resulted in **G** being formed as a major product. The spectrum of **G** [λ_{max} at pH 1.5 = 378, 355 (sh), 302, 274 (sh), 228 nm; Figure 6A] is quite different from those of **B** and dimers **C**–**F**. Cyclic voltammograms of **G** at pH 1.5 (Figure 6B) show a sharp reduction peak R_2 at −0.59 V and, on the reverse sweep, a quasi-reversible couple characterized by peaks O_2'/R_1' at 0.07 V. By use of the procedures described in the Experimental Section **G** was isolated as a bright yellow solid (molar mass 380 g, $C_{20}H_{20}N_4O_6$). In Me_2SO-d_6 the ^1H NMR spectrum of this compound is best explained by structure G_4 in Scheme II.

In order to gain additional evidence for the structure of **G**, it was electrochemically reduced at −0.75 V (peak R_2) in pH 1.5 HCl solution. Experimental n values of 2.0 ± 0.2 were measured. As the reduction proceeded, the yellow color and characteristic spectrum of **G** (Figure 6A) disappeared. The spectrum of the resulting product (λ_{max} in pH 1.5 HCl = 357, 341, 274 nm) is shown in Figure 7A. Oxidation of this colorless product solution at 0.15 V (or by exposure to air) caused the solution to become bright yellow-orange [λ_{max} = 434, 403, 386 (sh), 260 nm; Figure 7B]. Cyclic voltammetry on this solution (Figure 7C) showed a quasi-reversible couple at 0.07 V. Only the oxidized form of this couple could be isolated and was shown to be 4,4′-bi-[3-(2-aminoethyl)indolyliden-7-one] 5-5′-ether (**12**; Scheme III).

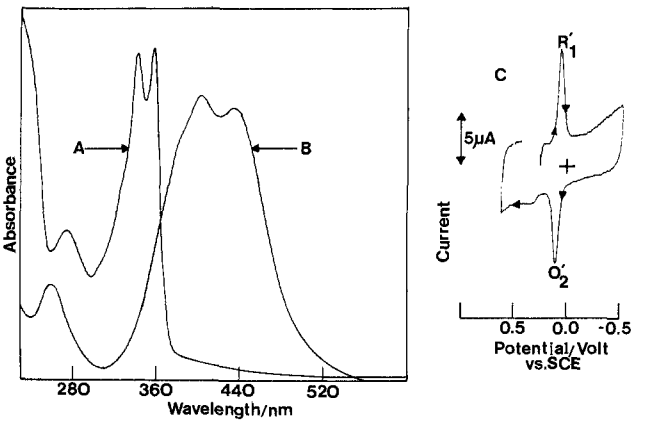

Figure 7. (A) Spectrum of **G** after controlled-potential electrochemical reduction at −0.75 V. This is the spectrum of 4,4′-bi-7-hydroxytryptamine] 5,5′-ether (**10**). (B) Spectrum after controlled-potential electrochemical oxidation of **10** at 0.15 V. This is the spectrum of 4,4′-bi-[3-(2-aminoethyl)indolyliden-7-one] 5,5′-ether (**11**). (C) Cyclic voltammogram at the PGE of the solution formed in (B). The samples in (A), (B), and (C) were dissolved in water adjusted to pH 1.5 with HCl. Sweep rate in (C), 200 mV s^{-1}.

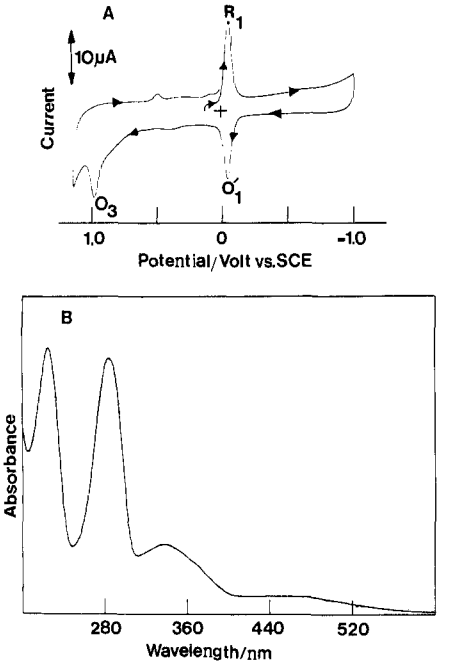

Figure 8. (A) Cyclic voltammogram at the PGE and (B) spectrum of 5-hydroxytryptamine-4,7-dione (**H**) in water adjusted to pH 1.5 with HCl. In (A) the sweep rate was 200 mV s^{-1}.

H was spectrally identified as 5-hydroxytryptamine-4,7-dione. The UV–visible spectrum of **H** is very characteristic (λ_{max} in pH 1.5 HCl = 461, 338, 283, 225 nm; Figure 8B). Cyclic voltammetry in pH 1.5 HCl (Figure 8A) shows that **H** is reversibly reduced at −0.07 V (peaks R_1/O_1'). It also shows oxidation peak O_3 at 0.97 V.

Discussion

Peaks O_1 and O_2 result from the primary, pH-dependent electrochemical oxidation of the neurotoxin 5,7-DHT. At pH 1.5 peak O_1 is an adsorption prepeak. However, peaks O_1 and O_2

do not simply represent an adsorption-controlled prepeak followed by the diffusion-controlled peak because controlled-potential electrolysis and cyclic voltammetry experiments clearly demonstrate that different products are formed at different potentials ranging from $E_{p/2}$ for peak O_1 to values more positive than E_p for peak O_2.

Electrooxidations of 5,7-DHT at potentials corresponding to $E_{p/2}$ for peak O_1 yield dimer **C** as the major product along with dimers **D**–**F**. These compounds all have the same molar mass (382 g) and hence must be simple dimers in which the 5,7-DHT residues are linked together at different positions. Formation of these simple dimers by low-potential electrooxidations of 5,7-DHT strongly suggests that the initial step in the reaction forms a radical intermediate. Electrolyses of 5,7-DHT at increasingly positive potentials causes first the yields of these simple dimers, particularly **C**, to decrease and the yield of **G**, which is the oxidation product of **C**, to increase. At even more positive potentials the monomer **H** replaces **C** and then **G** as the major product. This behavior suggests that at potentials greater than E_p for peak O_1 the primary radical intermediate is electrochemically oxidized. In view of the formation of several simple dimers upon low-potential oxidation it seems reasonable to propose that the primary reaction involves the $1e^-,1H^+$ oxidation of 5,7-DHT to form a radical represented as the resonance hybrid structure **4** [Scheme II; The structures marked with an asterisk in Schemes II and III were isolated and characterized by spectral methods (NMR, MS, UV–vis).] However, **C** is the predominant dimer formed which, based upon its facile oxidation to dimer **G**, must be 4,4′-bi-5,7-dihydroxytryptamine. Hence, the principal resonance form of radical **4** must be radical **5** in which the unpaired electron is located at the C(4) position. Dimerization of radical **5** would yield **6** and hence **C** as shown in Scheme II. The oxidation potential of **C** is such (Figure 4A) that electrolyses of 5,7-DHT at potentials close to E_p for peak O_1 cause **C** to be oxidized in an overall $2e^-,2H^+$ reaction to **G**. There are at least four tautomeric forms of **G** that can exist in solution, although in Me_2SO ^1H NMR spectra suggest that structure G_4 is the predominant form of this compound.

Under virtually all experimental conditions investigated 5-hydroxytryptamine-4,7-dione (**H**) is formed as a product of the electrochemical oxidation of 5,7-DHT at pH 1.5. However, the yield of **H** increases at more positive applied potentials and when low concentrations of 5,7-DHT are oxidized. Neither **C** nor **G** can be electrochemically oxidized to **H**, at least under the conditions used to oxidize 5,7-DHT. Since the conditions under which **H** becomes a major oxidation product are conditions that do not favor the formation of dimers, it seems clear that the only rational route to formation of the former compound must involve as a first step the oxidation ($1e^-,1H^+$) of radical **4** to the quinone imine **7** (Scheme II). Structure **7** represents only one of several resonance forms of this compound (see Scheme I). At pH 1.5 cyclic voltammetry of 5,7-DHT at sweep rates as fast as 20 V s^{-1} gives no evidence for a peak corresponding to the reduction of **7** (or indeed of putative radical **4**). This implies that **7** is a very reactive species and undergoes complete chemical transformation in less than 20 ms. This chemical transformation must involve the nucleophilic attack by water on **7** to yield 4,5,7-THT (Scheme II). This compound is more easily oxidized ($E^{\circ\prime} = -0.07$ V at pH 1.5) than 5,7-DHT, giving **H**. It is the **H**/4,5,7-THT couple that is responsible for quasi-reversible peaks R_1/O_1' observed in cyclic voltammograms of 5,7-DHT (Figure 1B). **H** is also responsible for oxidation peak O_3. However, the electrode reactions responsible for this peak remain to be determined.

In aqueous solution at pH 1.5, yellow dimer **G** is electrochemically reduced (peak R_2) in a $2e^-,2H^+$ reaction giving, ultimately, 4,4′-bi-[3-(2-aminoethyl)indolyliden-7-one] 5,5′-ether (**12**). Formation of **12** is easily rationalized by an initial $2e^-,2H^+$ reduction of the α,β-unsaturated ketone of G_4 to give **8** followed by the rapid loss of the elements of water yielding dimer **9**. The expected internal Michael reaction then forms ether **10** which rearranges to the symmetrical ether **11** as shown in Scheme III. The latter compound, 4,4′-bi′[7-hydroxytryptamine] 5,5′-ether, was difficult to isolate because of its ease of air oxidation. Air or electrochemical oxidation of **11** yields the yellow-orange ether **12**. Compounds **11** and **12** form the reversible couple responsible for peaks O_2'/R_1' observed in cyclic voltammograms of **G** (Figure 6B).

None of the separated or isolated products showed a reduction peak corresponding to peak R_3 observed in cyclic voltammograms of 5,7-DHT (Figure 1B). Accordingly, it must be concluded that the species responsible for this peak is an unstable precursor of identified products.

Conclusions

The results presented above establish that the primary electrochemical oxidation products of 5,7-DHT in acidic solution are reactive radical species and not a quinone imine intermediate. On the basis of the formation of dimer **C** (4,4′-bi-5,7-dihydroxytryptamine) as the major reaction product when 5,7-DHT is oxidized at low potentials, it may be concluded that the predominant form of the primary radical is **5** in which the unpaired electron is located at the C(4) position. This is, in fact, the key radical that Sinhababu and Borchardt[16] speculated to be formed in the primary step of autoxidation of 5,7-DHT.

A quinone imine intermediate is formed by the further electrochemical oxidation of the primary radical intermediate. The latter reaction only occurs to a major extent at potentials greater than or equal to E_p for voltammetric oxidation peak O_1 of 5,7-DHT.

The *p*-quinone of 4,5,7-THT, i.e., **H**, is a reasonably stable and relatively easily isolated compound. It is also worth noting that **H** is a more powerful neurotoxin than 5,7-DHT, although it lacks the selectivity of the latter compound.[18] The studies reported here were performed under conditions that are quite different from these found in the central nervous system. However, it is interesting to speculate that the selectivity of 5,7-DHT might indeed derive from its high-affinity uptake by the membrane pump of serotonergic neurons, whereas its neurodegenerative properties might be related to its oxidation to reactive radical intermediates or to the powerful neurotoxin **H**.

Acknowledgment. This work was supported by NIH Grant No. GM-32367-05. Additional support was provided by the Research Council and the Graduate College of the University of Oklahoma.

Registry No. 12, 117940-72-4; **C**, 117940-73-5; G_1, 117940-71-3; **H**, 100513-78-8; 5,7-DHT, 31363-74-3; 4,5,7-THT, 100513-77-7; graphite, 7782-42-5.